

# Electronic structure and phonons in $\text{La}_2\text{CoMnO}_6$ : A ferromagnetic insulator driven by Coulomb-assisted spin-orbit coupling

Santu Baidya and T. Saha-Dasgupta

*S.N. Bose National Centre for Basic Sciences, Kolkata 700098, India*

(Received 11 April 2011; published 29 July 2011)

Using first-principles density functional calculations, we study the electronic structure of double perovskite compound,  $\text{La}_2\text{CoMnO}_6$ , which is reported to be ferromagnetic insulator with a Curie temperature of about 240 K. Our calculations show that the insulating state in this compound is driven by Coulomb-assisted spin-orbit coupling operative within the Co-*d* manifold, with a rather large orbital moment of  $\approx 0.17 \mu_B$  at Co site. Motivated by the report of magnetodielectric behavior in this material, we also investigate the response of infrared active phonons to the underlying spin ordering. Our calculations exhibit existence of very soft phonon modes which show a substantially large response to the change in magnetic ordering, proving the existence of strong spin-phonon coupling in this material, as found in case of another related compound,  $\text{La}_2\text{NiMnO}_6$ .

DOI: [10.1103/PhysRevB.84.035131](https://doi.org/10.1103/PhysRevB.84.035131)

PACS number(s): 71.20.-b, 75.30.Et, 71.45.Gm

## I. INTRODUCTION

Ferromagnetic insulators are rare in nature. It is even more rare to find ferromagnetic insulators with relatively high Curie temperature which can be used for devices. Known examples, such as  $\text{EuO}$  ( $T_c \sim 77$  K),<sup>1</sup>  $\text{CdCr}_2\text{S}_4$  ( $T_c \sim 90$  K),<sup>2</sup>  $\text{SeCuO}_3$  ( $T_c \sim 25$  K) (Ref. 3) have Curie temperatures significantly below room temperature. Double perovskites bring lot of promises in this context. A few of them has been found to exhibit ferromagnetism as well as insulating properties with reasonably high Curie temperature, e.g.,  $\text{La}_2\text{NiMnO}_6$  ( $T_c \sim 280$  K),<sup>4</sup>  $\text{Sr}_2\text{CrOsO}_6$  ( $T_c \sim 700$  K).<sup>5</sup> For  $\text{La}_2\text{NiMnO}_6$ , additional interesting properties<sup>6</sup> such as magnetocapacitive behavior has been reported. Double perovskite compound  $\text{La}_2\text{CoMnO}_6$  (LCMO),<sup>7</sup> consisting of transition metal octahedra  $\text{CoO}_6$  and  $\text{MnO}_6$  has also been synthesized. Different studies on bulk and thin films of  $\text{La}_2\text{CoMnO}_6$  (LCMO) have carried during last years, exploring their properties. The precise valences of Co and Mn,<sup>8</sup> their spin states, the magnetic ground state have been a matter of debate.<sup>9</sup> Rigorous studies carried on bulk as well as thin films of LCMO on  $\text{SrTiO}_3$  substrate<sup>10,11</sup> have lead to the consensus that this diversity of the behavior presumably arises from the extend of ordering between Co and Mn. While Co/Mn ordered LCMO presents a ferromagnetic transition at  $T_c$  of about 240 K for disordered samples, a different transition occurs at about 150 K together with a spin-glass like behavior.<sup>12</sup> X-ray absorption spectroscopy (XAS) as well as x-ray absorption near-edge spectroscopy (XANES) experiments<sup>7,13</sup> suggested that ordered phases involve the 2+ and 4+ valences of Co and Mn, respectively, while the disorder phase is associated with 3+ and 3+ valences of Co and Mn, respectively. X-ray photoemission experiment carried out<sup>10</sup> on film of LCMO reported a total magnetic moment of  $5.7 \mu_B/\text{f.u.}$  suggesting the high spin states of both  $\text{Co}^{2+}$  and  $\text{Mn}^{4+}$  in the ordered state. We note that the high spin states of  $\text{Co}^{2+}$  and  $\text{Mn}^{4+}$  would indicate  $3d^7$  ( $t_{2g}^3 \uparrow t_{2g}^2 \downarrow e_g^2 \uparrow$ ) and  $3d^3$  ( $t_{2g}^3 \uparrow$ ) configuration, respectively. The spin-polarized density functional theory (DFT) calculations within the local density approximation (LDA) or generalized gradient approximation (GGA) of electron-electron correlation would result into metallic behavior in such

case. The observed insulating behavior in LCMO is therefore not so obvious as in  $\text{La}_2\text{NiMnO}_6$ . For  $\text{La}_2\text{NiMnO}_6$ , 2+ and 4+ valences of Ni and Mn lead to  $3d^8$  ( $t_{2g}^3 \uparrow t_{2g}^3 \downarrow e_g^2 \uparrow$ ) and  $3d^3$  ( $t_{2g}^3 \uparrow$ ) configuration, respectively, with either fully filled or empty states within a spin-polarized calculation. The origin of the insulating behavior in LCMO thus calls for the need of first-principles investigation. To the best of our knowledge, no first-principles electronic structure calculation exists for LCMO.

In this study, we report a detailed DFT study of the electronic structure of LCMO. For our calculation, we considered the rhombohedral crystal symmetry as reported for the high temperature phase of Co/Mn ordered samples.<sup>14</sup> We have also investigated the response of the phonon upon the magnetic ordering since the magnetocapacitive behavior has been reported for LCMO.<sup>15,16</sup>

The rest of the paper is organized as follows. In Sec. II, we present the details of our computational techniques. The results are presented in Sec. III, which consists of several subsections. Subsection III A describes the results on crystal structure, Subsection III B describes the results on the electronic and magnetic structure, while in Subsection III C, we report our obtained results on phonons and their coupling with spin. The concluding remarks are presented in Sec. IV.

## II. COMPUTATIONAL DETAILS

The calculations have been carried out using linear augmented plane wave (LAPW) basis with no shape approximation to the potential and charge density as implemented in WIEN2K (Ref. 17) as well as using the plane wave based pseudopotential method as implemented in VASP code.<sup>18</sup> For self-consistent calculations with LAPW basis, the number of  $k$  points were chosen to be 365. For the number of plane waves, the criterion used was muffin-tin radius multiplied by  $K_{\max}$  (for the plane wave) yielding a value of 7.0. In the La valence states,  $f$ -local orbital was added to reduce the linearization error. In the calculations involving spin-orbit coupling, it was included in scalar relativistic form as a perturbation to the original Hamiltonian. For the self-consistent calculation with the plane

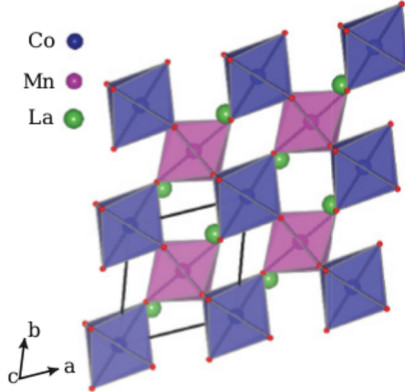


FIG. 1. (Color online) High-temperature crystal structure of  $\text{La}_2\text{CoMnO}_6$ . The violet (dark gray) and pink (light gray) colored octahedra denote the  $\text{CoO}_6$  and  $\text{MnO}_6$  octahedra, respectively. The La atoms shown as big balls sit in the hollow formed by  $\text{CoO}_6$  and  $\text{MnO}_6$  octahedra. The  $\text{CoO}_6$  and  $\text{MnO}_6$  octahedra connected by corner sharing O atom are tilted with respect to each other, with  $\text{Co}-\text{O}-\text{Mn}$  angle of about  $160^\circ$ . The rhombohedral unit cell of 1 f.u. is marked.

wave basis  $4 \times 4 \times 4$  Monkhorst-Pack  $k$  point mesh was used for good convergence and the energy cutoff was chosen to be 460 eV. The applied exchange-correlation functional was GGA in the Perdew and Wang (PW91) parametrization.<sup>19</sup> We used furthermore projector augmented wave (PAW) potentials.<sup>20</sup>

### III. RESULTS

#### A. Crystal structure

The rhombohedral unit cell of LCMO having lattice constant of 5.488 Å and 1 f.u. is shown in Fig. 1. In view of the fact that the positions of light atoms such as O, may not be well characterized within the experimental technique, we have carried out structural optimization where the internal degrees of freedom associated with La and O atoms have been optimized keeping the lattice parameters fixed at experimentally determined values.<sup>14</sup> The relaxed structural parameters

TABLE I. Energy-minimized structural parameters of LCMO. Lattice constants have been kept constant at the experimental values (Ref. 14).

| Space group = $R\bar{3}$ , $a$ (Å) = 5.488, $\alpha$ = 60.724 |                   |         |         |         |
|---|-------------------|---------|---------|---------|
| Atoms   | Wyckoff positions | X       | Y       | Z       |
| La  | 2c                | 0.25019 | 0.25019 | 0.25019 |
| Co  | 1a                | 0.0     | 0.0     | 0.0     |
| Mn  | 1b                | 0.5     | 0.5     | 0.5     |
| O   | 6f                | 0.80604 | 0.68227 | 0.25783 |

of the rhombohedral phase (see Table I) agree well within less than 1% with experimental ones. In the optimized structure, the  $\text{CoO}_6$  and  $\text{MnO}_6$  octahedra are regular having equal lengths of all Co–O and Mn–O bonds. The  $\text{CoO}_6$  and  $\text{MnO}_6$  octahedra though exhibit trigonal distortion, with O–Co–O angles and O–Mn–O angles differing from  $90^\circ$ . For  $\text{CoO}_6$  octahedra, they differ by  $1.31^\circ$  while for  $\text{MnO}_6$  octahedra, they differ by  $1.34^\circ$ . The Co–O–Mn angle is  $160.02^\circ$ , deviating significantly from  $180^\circ$  linear Co–O–Mn situation.

#### B. Electronic and magnetic structure

The spin-polarized density of states (DOS) calculated within GGA approximation in LAPW basis is shown in the left panel of Fig. 2. As we see, the electronic structure calculated within GGA approximation gives rise to a half-metallic solution, with a gap in the majority spin channel and finite density of states at the Fermi energy,  $E_F$ , in the minority spin channel. The transition metal  $d$ -oxygen  $p$  hybridized DOS extends from an energy range about  $-7$  eV below  $E_F$  to about 4 eV above  $E_F$ . While the low lying states occupying an energy range from about  $-7$  eV to about  $-4$  eV or  $-3$  eV are of predominant oxygen character, the states close to  $E_F$  are of predominant transition metal  $d$  character. The octahedral crystal field split  $\text{Mn-}t_{2g}$  states are occupied in the majority spin channel,  $\text{Mn-}e_g$  states being empty while both  $\text{Mn-}t_{2g}$  and  $\text{Mn-}e_g$  states are empty in the minority spin channel. Both  $\text{Co-}t_{2g}$  and  $\text{Co-}e_g$  states are occupied in the majority

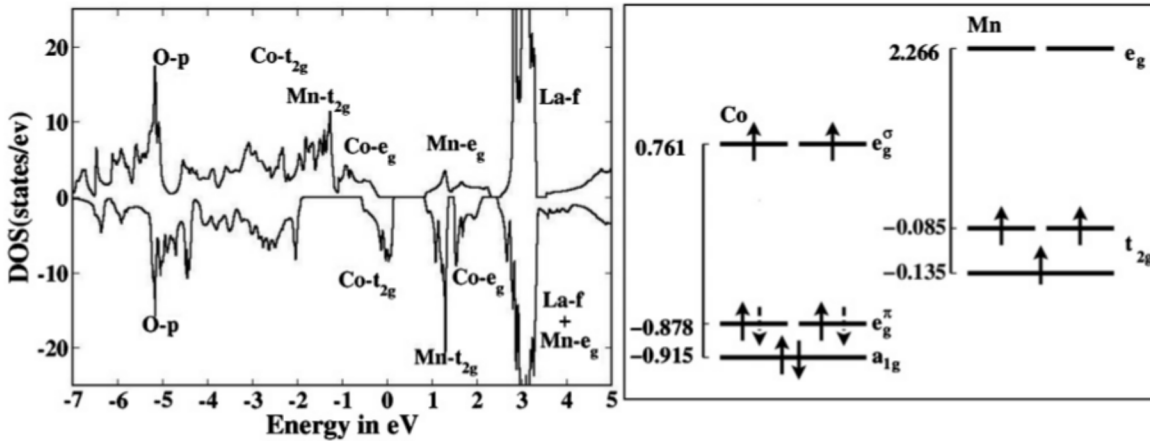


FIG. 2. (Left panel) Spin-polarized density of states calculated within GGA in the geometry optimized rhombohedral phase. The dominant orbital contributions are marked. Zero of the energy is set at the GGA Fermi energy. (Right panel) The energy levels of Co and Mn  $d$  levels in eV unit and their nominal occupancies.

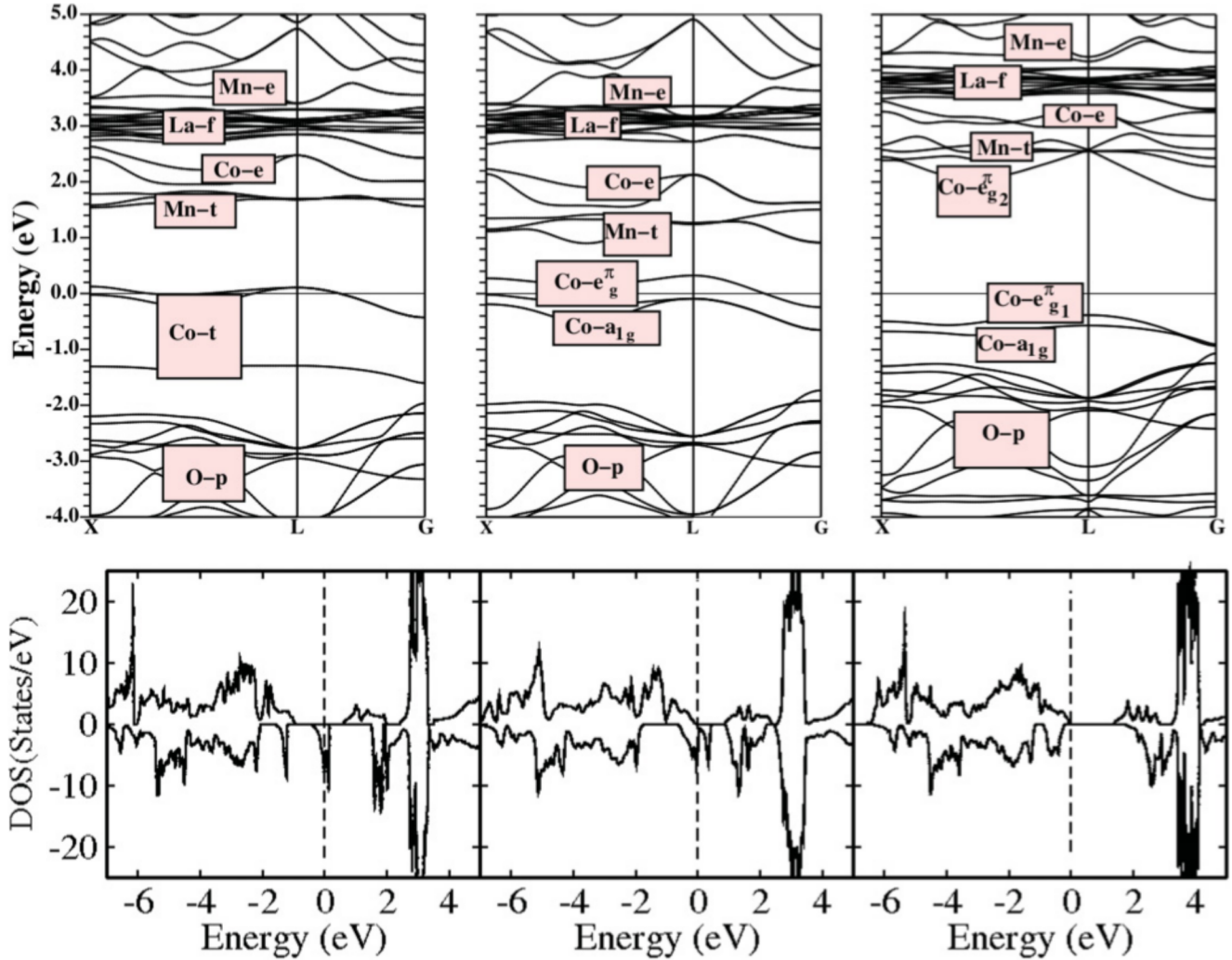


FIG. 3. (Color online) (Upper panels) Band structure in the minority spin channel. Energies are plotted with respect to  $E_F$  in eV unit. (From left to right) Band structures calculated with GGA +  $U$ , GGA + SO and GGA +  $U$  + SO, respectively. In the GGA +  $U$  and GGA +  $U$  + SO calculations, the  $U$  and  $J_H$  values were chosen as  $U = 4.0$  eV and  $J_H = 0.9$  eV. For the SO calculations, the spin quantization axis was chosen as [001]. (Lower panels) Corresponding density of states.

spin channel while partially filled  $\text{Co-}t_{2g}$  states cross  $E_F$  in the minority spin channel, minority  $\text{Co-}e_g$  states being empty. This result is in agreement with nominal valences of  $\text{Co}^{2+}$  and  $\text{Mn}^{4+}$  as reported in Refs. 7, 13, and 14. In accordance with the half metallic nature of the solution, the total magnetic moment turned out to be of integer value of  $6.0 \mu_B/\text{f.u.}$  with  $0.01 \mu_B$  at La site,  $2.42 \mu_B$  at Co site,  $2.74 \mu_B$  at Mn site,  $0.09 \mu_B$  at O site, and rest residing in the interstitial. The right panel of Fig. 2 shows the  $d$ -energy level positions at Co and Mn sites, measured with respect to  $E_F$  in non-spin-polarized situation. The octahedral crystal field splits the five-fold degenerate  $d$  levels into broad grouping of low-lying  $t_{2g}$ 's and high-lying  $e_g(e_g^\sigma)$ 's. The presence of additional trigonal distortion in the  $\text{CoO}_6$  and  $\text{MnO}_6$  octahedra further splits the  $t_{2g}$  states into singly degenerate  $a_{1g}$  and doubly degenerate  $e_g^\pi$ 's, with  $e_g^\pi$ 's being higher in energy compared to  $a_{1g}$ . The half metallic solution obtained within the spin-polarized GGA calculation is therefore obvious. The states in the majority spin channel are either fully empty or occupied. In the minority spin channel out of  $2e^-$ 's at the Co site, one occupies lowest lying  $a_{1g}$  state

and the remaining  $e^-$  can occupy either of the any doubly degenerate  $e_g^\pi$  states giving rise to a partially filled situation. While the broad  $t_{2g}-e_g$  splittings turn out to be about 2 eV,  $a_{1g}-e_g^\pi$  splittings are much smaller,  $\approx 0.04\text{--}0.05$  eV.

Application of missing correlation effect in the form of GGA +  $U$  calculation though increases the splitting between occupied  $\text{Co-}e_g$  and unoccupied  $\text{Mn-}e_g$  states in the majority spin channel, and that between occupied  $\text{Co-}t_{2g}$  and empty  $\text{Mn-}t_{2g}$ ,  $\text{Co-}e_g$  in the minority spin channel, it cannot lift the degeneracy between degenerate  $\text{Co-}e_g^\pi$  states in the minority spin channel, leaving them partially filled with one electron. The left most upper panel of Fig. 3 shows the band structure of LCMO calculated within GGA +  $U$  (Ref. 21) for a typical choice of  $U = 4$  eV and  $J_H = 1$  eV applied at Co and Mn sites. Only the minority channel is shown, since the majority channel is already gaped with either completely occupied or empty states. The corresponding DOS for both the spin channels is shown in the left most lower panel.

In order to explore the effect of spin-orbit coupling which is operative in  $t_{2g}$  manifold, we carried out GGA + SO

TABLE II. Magnetic moments of Co and Mn ions in  $\mu_B$ .

|                | Co             |             | Mn             |             |
|----------------|----------------|-------------|----------------|-------------|
|                | Orbital moment | Spin moment | Orbital moment | Spin moment |
| GGA            | ...            | 2.421       | ...            | 2.735       |
| GGA + $U$      | ...            | 2.572       | ...            | 2.830       |
| GGA + SO       | 0.135          | 2.405       | -0.012         | 2.761       |
| GGA + $U$ + SO | 0.169          | 2.555       | -0.018         | 2.877       |

calculations for LCMO with the magnetization axis chosen along [001] direction. The orbital moment at Co and Mn site turned out to be  $0.14 \mu_B$  and  $-0.01 \mu_B$ , respectively.  $\text{Co}^{2+}$  being more than half filled, the orbital moment is pointed along the direction of the spin moment, while  $\text{Mn}^{4+}$  being less than half filled, the orbital moment is pointed opposite to the direction of spin moment as listed in Table II. The orbital moment at Mn site is tiny due to the  $t_{2g}^3$  configuration with no orbital degrees of freedom left. The orbital moment at the Co site, on the other hand, is large due to the orbitally degenerate  $e_g^\pi$  states and introduction of SO coupling lifts the degeneracy of  $e_g^\pi$  as shown in upper middle panel of Fig. 3. This lifting of degeneracy gives rise to a pseudogap at  $E_F$  in the density of states in the minority spin channel, failing a bit short of opening the gap, as shown in the lower middle panel. The situation changes significantly upon application of GGA +  $U$  + SO, as is shown in the last panels of Fig. 3. For choices of  $U = 4.0 \text{ eV}$  and  $J_H = 1.0 \text{ eV}$ , the orbital moment at Co site was renormalized to a value of  $0.17 \mu_B$ . The Mn orbital moment also showed a small renormalization to a value of  $-0.02 \mu_B$ . This makes  $\text{Co}-e_{g,1}^\pi$  state completely occupied and  $\text{Co}-e_{g,2}^\pi$  state completely empty in the minority spin channel, opening up a gap of about  $1.7 \text{ eV}$ .<sup>22</sup> This clearly exhibits that LCMO is an insulator driven by Coulomb-assisted spin-orbit coupling, as has also been recently found for spinel compound<sup>23</sup>  $\text{Fe}_2\text{CrS}_4$ , and another double perovskite compound<sup>24</sup>  $\text{Ba}_2\text{NaOsO}_6$ .

Within the spin-polarized calculations, the ferromagnetic spin alignment between Co and Mn, was found to be energetically stabler compared to antiferromagnetic spin alignment by about  $0.3 \text{ eV}$ , in conformity with the observed ferromagnetism in this compound.<sup>7</sup> The antiparallel alignment leads to a total spin of zero, with perfect cancellation of Co and Mn spins. Constructing a low-energy Hamiltonian in terms of Co- $d$  and Mn- $d$  degrees of freedom using the  $N$ th order muffin-tin orbital (NMTO) based downfolding<sup>25</sup> calculations and employing the extended Kugel-Khomskii-like model (Ref. 26), as done for<sup>27</sup>  $\text{La}_2\text{NiMnO}_6$ , the nearest neighbor magnetic exchange interaction between Co and Mn turned out to be of ferromagnetic nature and a value of  $4 \text{ meV}$ , for a choice of  $U = 4.0 \text{ eV}$  and  $J_H = 1.0 \text{ eV}$ .

### C. Phonons

LCMO compound has been reported to exhibit magnetodielectric effect.<sup>15</sup> In order to investigate this issue, we studied the response of optimized rhombohedral structure to changes in magnetic ordering, e.g., changes in phonon frequencies with changes in magnetic ordering. For this purpose, we calculated the  $\Gamma$ -point phonons for the rhombohedral structure for the

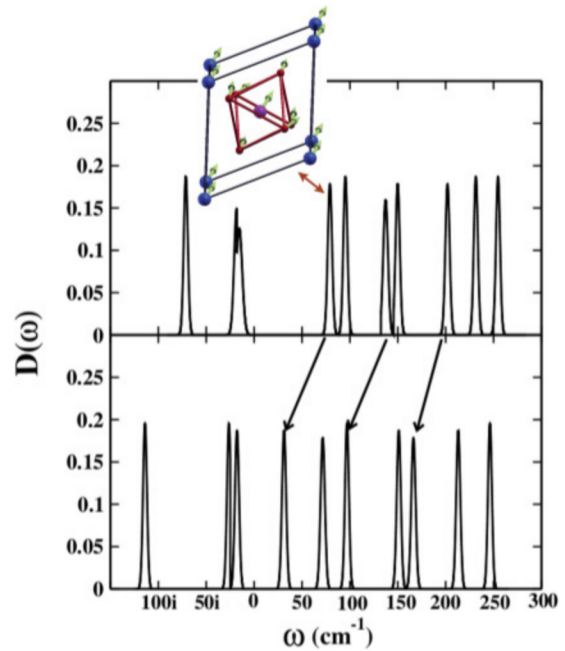


FIG. 4. (Color online) Phonon spectra of rhombohedral LCMO considering the ferromagnetic (top panel) and antiferromagnetic (bottom panel) alignment of Co and Mn spins. The arrows show the shifting of dominant IR active phonon modes. The inset shows the displacement of atoms corresponding to the lowest frequency IR-active mode. The La atoms have been omitted for clarity.

ferromagnetic alignment of Co and Mn spins *vis-à-vis* the antiparallel alignment of Co and Mn spins. Since the considered rhombohedral structure is the high temperature structure while the ground state structure is of monoclinic symmetry,<sup>14</sup> our  $T = 0 \text{ K}$  calculations carried out on rhombohedral symmetry show presence of unstable modes. We find that frequencies of the lowest energy infrared (IR)-active phonons soften from  $79.1$ ,  $137.3$ , and  $201 \text{ cm}^{-1}$  in the FM phase to  $31.2$ ,  $96.9$ , and  $166.3 \text{ cm}^{-1}$ , respectively (indicated by arrows in Fig. 4), exhibiting a strong coupling with spin. The examination of atomic displacements corresponding to the lowest frequency mode, as shown in the inset of Fig. 4, shows that the angle between the Mn-O (at the center of the oxygen-octahedra) and O-Co (rightmost corner of the cell) is affected by this phonon, reflecting the signature of exchange-striction driven spin-phonon coupling. Such softening of phonon modes in the vicinity of magnetic phase transition was also observed for Raman-active phonons in the measurement<sup>15</sup> by Truong *et al.*, revealing a strong spin-lattice coupling in LCMO. Our observed softening of IR-active phonon modes may be compared with the case of  $\text{La}_2\text{NiMnO}_6$ , where softest phonon was found<sup>27</sup> to soften from  $91.3 \text{ cm}^{-1}$  in FM phase to  $65.5 \text{ cm}^{-1}$  for the antiparallel alignment. One would therefore expect a similar nature of magnetodielectric effect in LCMO as observed in case of  $\text{La}_2\text{NiMnO}_6$ . We note that neither of these two double perovskites are ferroelectrics. If they can be made ferroelectric by doping<sup>28</sup> or straining then one would expect a new class of multiferroic material with large magnetoelectric effect.

#### IV. CONCLUSION

In conclusion, using first-principles DFT calculations, we have explored the electronic structure of FM double perovskite compound, LCMO, which to the best of our knowledge has not been taken up earlier. Our study shows that unlike the sister compound,  $\text{La}_2\text{NiMnO}_6$ , the insulating behavior in this compound, is driven by spin-orbit coupling within the  $\text{Co}-e_g^\pi$  states of the octahedral and trigonal crystal field split  $\text{Co}-d$  manifold which gets assisted by the presence of Coulomb correlation. We also explored the existence of possible spin-

phonon coupling in this material. Our study showed the presence of soft IR-active phonon modes that respond strongly in terms of further softening upon changing the magnetic ordering. This would lead to large magnetodielectric effect, as observed experimentally.

#### ACKNOWLEDGMENT

T.S.D. acknowledges funding through DST projects. The authors acknowledge P. S. Anil Kumar for discussion.

- 
- <sup>1</sup>B. T. Matthias, R. M. Bozorth, and J. H. Van Vleck, *Phys. Rev. Lett.* **7**, 160 (1961).
- <sup>2</sup>P. K. Baltzer, H. W. Lehmann, and M. Robbins, *Phys. Rev. Lett.* **15**, 493 (1965).
- <sup>3</sup>M. A. Subramanian, A. P. Ramirez, and W. J. Marshall, *Phys. Rev. Lett.* **82**, 1558 (1999).
- <sup>4</sup>A. Wold, R. J. Arnott, and J. B. Goodenough, *J. Appl. Phys.* **29**, 387 (1958).
- <sup>5</sup>Y. Krockenberger, K. Mogare, M. Reehuis, M. Tovar, M. Jansen, G. Vaitheswaran, V. Kanchana, F. Bultmark, A. Delin, F. Wilhelm, A. Rogalev, A. Winkler, and L. Alff, *Phys. Rev. B* **75**, 020404 (2007).
- <sup>6</sup>N. S. Rogado, J. Li, A. W. Sleight, and M. A. Subramanian, *Adv. Mater.* **17**, 2225 (2005).
- <sup>7</sup>V. L. Joseph Joly, Y. B. Khollam, P. A. Joy, C. S. Gopinath, and S. K. Date, *J. Phys. Condens. Matter* **13**, 11001 (2001).
- <sup>8</sup>K. Asai, H. Sekizawa, and S. Iida, *J. Phys. Soc. Jpn.* **47**, 1054 (1979); A. Wold, R. J. Arnott, and J. B. Goodenough, *J. Appl. Phys.* **29**, 387 (1958).
- <sup>9</sup>M. P. Singh, K. D. Truong, and P. Fournier, *Appl. Phys. Lett.* **91**, 042504 (2007); R. I. Dass and J. B. Goodenough, *Phys. Rev. B* **67**, 014401 (2003).
- <sup>10</sup>H. Z. Guo, A. Gupta, T. G. Calvarese, and M. A. Subramanian, *Appl. Phys. Lett.* **89**, 262503 (2006).
- <sup>11</sup>P. A. Joy, Y. B. Khollam, and S. K. Date, *Phys. Rev. B* **62**, 8608 (2000); M. P. Singh, K. D. Truong, and P. Fournier, *Appl. Phys. Lett.* **91**, 042504 (2007).
- <sup>12</sup>A. J. Barón-González, C. Frontera, J. L. García-Muñoz, J. Roqueta, and J. Santiso, *J. Phys.: Conf. Ser.* **200**, 092002 (2010).
- <sup>13</sup>T. Kyômen, R. Yamazaki, and M. Itoh, *Chem. Mater.* **15**, 4798 (2003).
- <sup>14</sup>C. L. Bull, D. Gleeson, and K. S. Knight, *J. Phys. Condens. Matter* **15**, 4927 (2003).
- <sup>15</sup>K. D. Truong, J. Laverdiére, M. P. Singh, S. Jandl, and P. Fournier, *Phys. Rev. B* **76**, 132413 (2007).
- <sup>16</sup>S. Yanez-Vilar, A. Castro-Couceiro, B. Rivas-Murias, A. Fondado, J. Mira, J. Rivas, and M. A. Senaris-Rodriguez, *Z. Anorg. Allg. Chem.* **631**, 2265 (2005); Y. Lin and X. Chen, *J. Am. Ceram. Soc.* **94**, 782 (2011).
- <sup>17</sup>P. Blaha, K. Schwartz, G. K. H. Madsen, D. Kvasnicka, and J. Luitz, Full-potential LAPW code WIEN2K.
- <sup>18</sup>G. Kresse and J. Hafner, *Phys. Rev. B* **47**, R558 (1993); G. Kresse and J. Furthmüller, *ibid.* **54**, 11169 (1996).
- <sup>19</sup>J. P. Perdew, J. A. Chevary, S. H. Vosko, Koblar A. Jackson, Mark R. Pederson, D. J. Singh, and Carlos Fiolhais, *Phys. Rev. B* **46**, 6671 (1992).
- <sup>20</sup>P. E. Blöchl, *Phys. Rev. B* **50**, 17953 (1994); G. Kresse and D. Joubert, *ibid.* **59**, 1758 (1999).
- <sup>21</sup>V. I. Anisimov, I. V. Solovyev, M. A. Korotin, M. T. Czyzyk, and G. A. Sawatzky, *Phys. Rev. B* **48**, 16929 (1993).
- <sup>22</sup>The gap value is found to increase more or less linearly upon increasing U value. To the best of our knowledge, no experimental estimate of gap value exists in literature. While the U value has been chosen to be typical U values for Co and Mn, it may be adjusted following the knowledge of the experimental gap value.
- <sup>23</sup>S. Sarkar, M. De Raychaudhury, I. Dasgupta, and T. Saha-Dasgupta, *Phys. Rev. B* **80**, 201101 (2009).
- <sup>24</sup>H. J. Xiang and M.-H. Whangbo, *Phys. Rev. B* **75**, 052407 (2007).
- <sup>25</sup>O. K. Andersen and T. Saha-Dasgupta, *Phys. Rev. B* **62**, R16219 (2000).
- <sup>26</sup>K. I. Kugel and D. I. Khomskii, *Sov. Phys. Usp.* **25**, 231 (1982).
- <sup>27</sup>H. Das, U. V. Waghmare, T. Saha-Dasgupta, and D. D. Sarma, *Phys. Rev. Lett.* **100**, 186402 (2008).
- <sup>28</sup>D. J. Singh and C. H. Park, *Phys. Rev. Lett.* **100**, 087601 (2008).